

Inclusions of Unusual Late Magmatic Melts in Quartz from the Oktyabr'skaya Pegmatite Vein, Malkhan Field (Central Transbaikal Region)

S. Z. Smirnov¹, I. S. Peretyazhko², V. E. Zagorsky², and M. Yu. Mikhailov¹

Presented by Academician N.V. Sobolev March 21, 2003

Received April 8, 2003

The primary magmatic origin of the majority of granitic pegmatites is beyond question. The *PT* parameters of the magmatic stage are best known for rock crystal and topaz–beryl (with sub-rare-metals) pegmatites [1, 2]. They are also known for pegmatites at the Ehrenfriedersdorf Sn–W deposit in Saxony [3]. Some evidence for crystallization conditions of rare metal miarolitic (with sub-rare-metals) [1, 4] and rare metal [5] pegmatites is also available. We began the systematic studies of mineral-forming media in order to estimate the role of volatile components and rare elements in the formation of granitic pegmatites with different specializations. In particular, we established the important role of orthoboric acid in the formation of miarolitic pegmatites enriched or depleted in boric mineralization [6, 7].

In this communication, we report new data on the late magmatic stage of the Oktyabr'skaya Vein localized in the Malkhan field (central Transbaikal region). It serves as an economic source of jewelry- and collection-grade tourmaline [8]. The Oktyabr'skaya Vein is a gently dipping lenticular pegmatite body, 250 m long and up to 17 m thick, hosted in metadiorites. The pegmatite is composed of intercalating graphic and sub-graphic quartz–K-feldspar and quartz–oligoclase mineral assemblages with subordinate pegmatoid quartz–feldspar segregations increasing toward the vein center. The K-feldspar becomes more abundant relative to oligoclase in the same direction. All pegmatite varieties contain subordinate coarse-crystalline schorl (locally abundant) and the presence of cavities from several cubic centimeters to a few cubic meters in volume. Quartz, K-feldspar, cleavelandite, lepidolite, colored

tourmaline, danburite, and hambergite are major minerals of the drusy assemblage. The mineral composition of the drusy material and degree of cavity filling are variable. Many cavities are surrounded by discrete tourmaline–lepidolite–albite rims (zones). A small equant cavity (maximal diameter ~15 cm) was chosen for the detailed investigation. The drusy assemblage in this cavity contains crystals of smoky quartz, druses of white cleavelandite, and a few K-feldspar and pink tourmaline crystals. Grains of black cassiterite, up to 3 × 5 mm in size, occur at the base of one feldspar crystal. A pale blue apatite crystal (0.3 × 1.0 cm) associated with pink tourmaline (0.6 × 1.0 cm), cleavelandite, and smoky quartz was observed on the cavity wall. The faces of some crystals are coated by a crust of fine-flaky lepidolite, 2–3 mm thick. Minerals of the drusy assemblage grow over the coarse-grained quartz–plagioclase (albite + oligoclase) pegmatite zone (1–2 cm) that grades into the medium-grained, locally graphic quartz–oligoclase pegmatite with sporadic schorl grains, 2–3 mm in size. The host pegmatite contains zircon, topaz, beryl, and apatite inclusions, unidentified rare metal phosphate, Ta- and Nb-bearing cassiterite, columbite, wolframite, and Fe–Mn wolframotantaloniobate, (close in composition to wolframixiolite).

Characteristics of melt and fluid inclusions.

Quartz from the host coarse- and medium-grained pegmatite contains small (1–10 μm) melt inclusions (MI), associated primary fluid inclusions (FI) 5–15 μm in size, and secondary FI (up to 20 μm). The quartz crystals freely overgrowing the cavity walls also contain melt inclusions (30–50 μm, occasionally more than 100 μm) together with primary (100 μm and more) and secondary fluid inclusions. In our case, inclusions irregularly distributed within the host quartz were considered primary. Fluid inclusions found within the same clusters with melt inclusions were considered cogenetic with respect to the melt inclusions. The melt inclusions in quartz from pegmatite zones around the cavity and at the base of drusy quartz crystals are mainly crystalline aggregate. The fluid phase is poorly discernible in the interstitial space of the crystalline aggregate (Fig. 1a).

¹ Institute of Mineralogy and Petrography, Siberian Division, Russian Academy of Sciences, pr. akademika Koptyuga 3, Novosibirsk, 630090 Russia
e-mail: ssmr@uiggm.nsc.ru

² Vinogradov Institute of Geochemistry, Siberian Division, Russian Academy of Sciences, ul. Favor'skogo 1a, Irkutsk, 650033 Russia

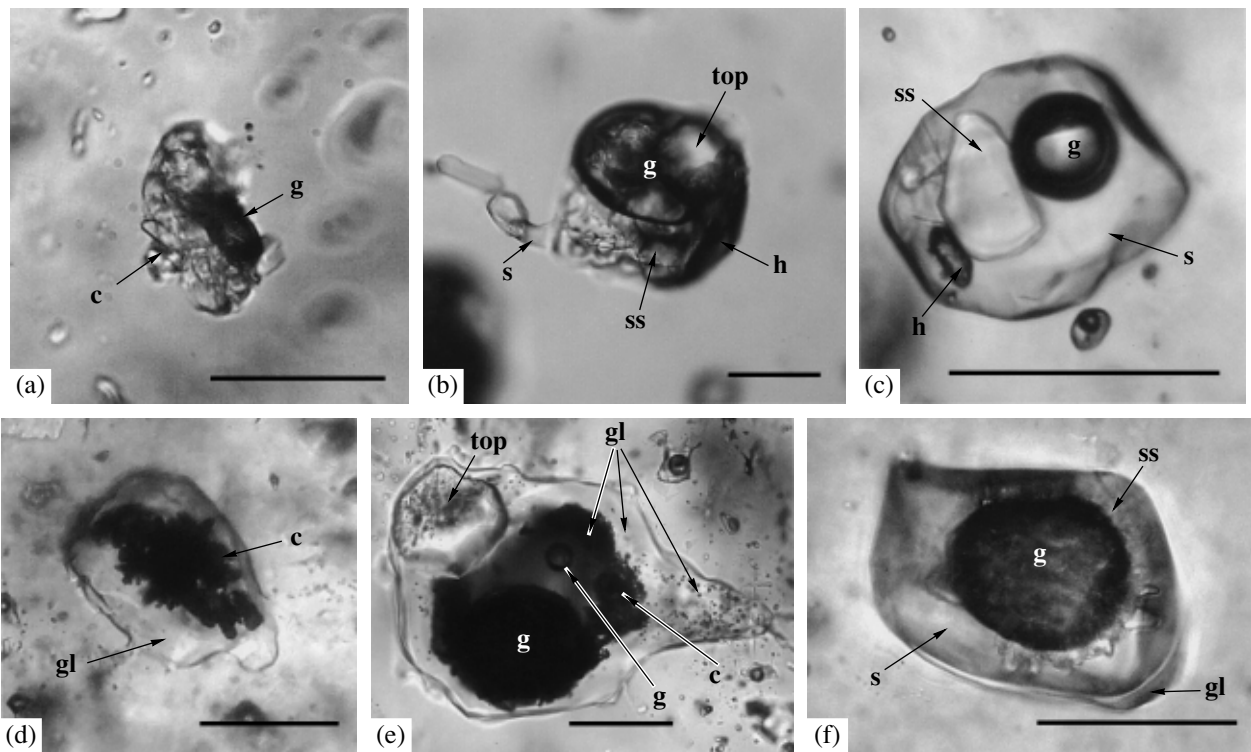


Fig. 1. Melt and fluid inclusions in quartz from miarolitic pegmatite in the Oktyabr'skaya Vein. Inclusions before heating in autoclave: (a) crystalline melt inclusion, (b) melt inclusion with abundant fluid phase; (c) fluid inclusion with unidentified crystalline phase. Inclusions after heating in autoclave at 640°C and 2.5 kbar: (d) melt inclusion with glass and unmelted crystalline phase (muscovite); (e) melt inclusion containing glass, small gas segregations, and unmelted topaz and muscovite; (f) nonhomogenized inclusion with glass and fluid segregation (hydrous solution + gas + sassolite). (c) Muscovite–lepidolite–nanpingite crystalline aggregate; (top) topaz; (gl) glass; (s) hydrous solution; (g) gas bubble; (ss) sassolite. The scale bar is 50 μm .

The amount of fluid phase in melt inclusions notably increases from older to younger generations of drusy quartz. The liquid, sassolite (H_3BO_3) crystals, and gas bubble are clearly seen within the fluid phase of some inclusions. The MI content abruptly diminishes from the early to intermediate growth zones, and fluid inclusions become predominant. In addition to sassolite, unidentified daughter crystals are found in some fluid inclusions (Fig. 1c). No melt inclusions were detected in the late growth zones. The volumetric proportions of crystalline aggregate, solution, and gas widely vary even in neighboring melt inclusions. This is probably related to heterogeneous entrapment of coexisting melt and fluid by the host mineral.

Based on Raman spectroscopy, the crystalline aggregate of melt inclusions within the drusy quartz largely consists of micaceous minerals with muscovite and lepidolite structure. The mica composition was determined by microprobe analysis in several opened melt inclusions. The high dispersion of F and especially Cs contents is typical (Table 1). The Cs content significantly increases (up to 20–24 wt %) toward the mica flake margins. Judging from the available analytical data, the micaceous aggregate is a mixture of muscovite, Cs-rich muscovite or nanpingite $\text{CsAl}_2[\text{AlSi}_3\text{O}_{10}](\text{OH},\text{F})_2$, probably B-rich muscovite

varieties, and lepidolite. Based on EMPA and SEM EDS data, the crystalline aggregate of many melt inclusions also contain topaz (table 1, analysis 1), quartz, K-feldspar, probably tourmaline (based on optic properties), and several unspecified minerals. The Raman spectra of melt inclusions without visible fluid phase always contain the 880 cm^{-1} line, suggesting the presence of orthoboric acid and small sassolite crystals in the interstitial space of crystalline aggregates. Cogenetic fluid inclusions contain aqueous boric acid solution, gas bubble, and one or several daughter sassolite crystals.

The behavior of small (1–2 μm) melt inclusions in quartz from the coarse-grained pegmatite and the cavity during heating was studied under atmospheric pressure using the heating stage and quenching technique [9]. The crystalline aggregate started to melt at 550–580°C, and the majority of inclusions homogenized at 600–610°C. Large melt inclusions were homogenized under external water pressure in autoclave with a cold seal. A flat polished quartz plate was placed in the copper insert (volume 1.5 cm^3). The plates were held at 500, 550, 600, and 650°C ($\pm 10^\circ\text{C}$) and 2.5 kbar for 14–24 h. Incipient melting of the drusy quartz was detected at 500–550°C. Complete melting of the last silicate phases was established only in some large melt inclu-

Table 1. Average chemical compositions of daughter phases in crystalline aggregate of melt inclusions, wt %

Component	1(5)	2(8)	3(2)	4(4)	5(7)
SiO ₂	32.89	45.67	39.63	40.90	43.08
Al ₂ O ₃	56.30	31.40	26.05	19.66	16.02
CaO	0.00	0.01	0.06	0.12	0.02
FeO	0.00	0.00	0.00	0.00	0.00
MnO	–	0.00	0.01	0.04	0.04
Na ₂ O	0.01	0.45	0.99	0.77	0.22
K ₂ O	0.00	10.33	5.95	3.56	1.76
Rb ₂ O	0.00	0.21	0.23	0.23	0.26
Cs ₂ O	0.01	0.18	5.71	15.06	22.66
F	18.11	1.78	2.40	5.11	6.70
Σ(–O=F ₂)	99.69	89.28	80.01	83.18	87.94

Notes: (1) Topaz; (2–5) probably B-rich micas of the muscovite–nanpingite series. Number of analyses is shown in parentheses. Minerals were analyzed with a Camebax-Micro microprobe at the Institute of Mineralogy and Petrography, Novosibirsk (L.N. Pospelova, analyst).

sions at 615°C. Microthermometric data on fluid inclusions and fluid phases in melt inclusions from drusy quartz are presented in Table 2. The table also shows estimates of H₃BO₃ and NaCl concentrations (equiv %) in homogeneous solutions determined with technique reported in [6, 7].

After heating in autoclave and rapid quenching, the inclusions in drusy quartz plates contained glass and muscovite and topaz crystals (Figs. 1d, 1e), or glass, solution, and gas bubble surrounded with a dense corona of sassolite crystals in variable volumetric proportions (Fig. 1f). In the absence of leakage, the rise of homogenization temperature for fluid segregation in melt inclusions from 250–300 to 350°C testifies to the decrease in fluid phase density, most likely due to water dissolution in melt. After heating in autoclave, the microthermometric properties of fluid in melt inclusions remained virtually unchanged (Table 2). The composition of quenched glass in melt inclusions was studied by the EMPA and SIMS methods (Table 3). The glass is characterized by unusually high Cs, F, B, and H₂O contents, with almost a complete lack of femic components, Cl, and P. Low Na contents (Table 3, anal-

yses 1–3) likely indicate a loss of this element during the analysis of hydrous aluminosilicate glass. Following the recommendations in [10], we tried to reduce the loss with the help of a defocused (20 μm) microprobe beam and beam current of 10 nA. As a result, the Na₂O content increased severalfold and reached 1.41 wt % (Table 3, analysis 4). Based on SIMS data, the glass also contains Li, Be, Ta, and Nb. However, even taking the SIMS data on the contents of light elements and water (5.67 wt %) into account, the analytical total remains much lower than 100% (Table 3, analysis 4). It seems likely that the low sum is caused by the loss of water during the analysis of glass. As was shown in [11], when the H₂O content in glass is higher than 5 wt %, the uncertainty of determination with SIMS technique markedly increases, probably due to the contribution of molecular H₂O. Hence, the H₂O content in the glass of melt inclusions can reach 12–15 wt %. Because boron in such glass largely occurs as B(OH)₃ [12], one can suggest that this element was also partly lost along with water vapor owing to the high volatility of orthoboric acid coupled with water vapor. Thus, boron concentrations in MI glasses obtained by the SIMS analysis are probably underestimated.

Discussion. Data on the composition and crystallization conditions of melts at the late magmatic stage of pegmatite formation remains scanty. According to [1, 2], the late melts of intragranitic rock crystal and topaz–beryl miarolitic pegmatites are derived from deeply evolved granitic magma saturated with volatile components. Recent experiments have shown that aluminosilicate melts enriched in F, B, and P and depleted in silica (relative to granite) can coexist under certain *PT* conditions with hydrous fluid and hydrous salt melt (high-temperature brine), i.e., with high-water and low-silicic aluminoborosilicate melts [12].

Cogenetic melt and fluid inclusions in quartz from the cavity-enclosing oligoclase pegmatite and the base of drusy quartz crystals indicate that the quartz–feldspar walls of the cavity, as well as the early zones of drusy quartz, crystallized from a heterogeneous mineral-forming medium with a gradually increasing fluid/melt ratio. The end of magmatic crystallization and onset of hydrothermal stage are fixed by the disappearance of melt inclusions associated with fluid inclusions in intermediate and late growth zones of miarolitic quartz. Judging from the MI homogenization data,

Table 2. Microthermometric characteristics of fluid inclusions and fluid segregations in melt inclusions from drusy quartz

Object	<i>T</i> _{eut} , °C	<i>T</i> _{i. m.} , °C	<i>T</i> _{ss} , °C	<i>T</i> _{hom} , °C	<i>C</i> _{H₃BO₃} , wt %	<i>C</i> _{NaCl equiv} , wt %
Fluid inclusions	–6.5...–28	–2.9...–6.5	59–88	220–360	12–20	4.6–9.4
Fluid segregations in melt inclusions	–9.5	–3.7...–7.6	70–80	250–300	15–17	5.7–9
		–4.2*	72*	350–335*	15.4*	5.4*

Notes: (ss) Sossolite; (eut) eutectic; (i. m.) ice melting; (hom) homogenization. (*) After heating and quenching in autoclave. H₃BO₃ and NaCl were determined by the method described in [6, 7].

Table 3. Chemical composition of quenched glass in melt inclusions, wt %

Component	1	2	3	4	5	6
SiO ₂	58.26	58.81	57.55	58.21	56.9	60.07
Al ₂ O ₃	12.59	13.06	12.64	12.62	11.4	17.85
CaO	0.08	0.03	0.16	0.16	0.03	0.04
FeO	b.d.	b.d.			0.24	0.17
MnO	b.d.	b.d.			0.04	0.02
BeO				0.12	0.30	0.08
Na ₂ O	0.51	0.27	0.61	1.41	2.04	4.97
K ₂ O	2.58	1.77	3.29	4.10	4.33	4.00
Rb ₂ O	0.10	0.10	0.05	0.14	1.10	0.44
Cs ₂ O	4.46	3.64	4.77	5.20	1.59	0.07
Li ₂ O				0.54	0.57	0.14
B ₂ O ₃				2.51	3.70	0.08
Ta ₂ O ₅				0.57		
Nb ₂ O ₅				0.10		0.01
P ₂ O ₅				n.d.	1.14	0.00
F	1.94	2.36	2.63	2.73	2.45	5.11
Cl	b.d.	b.d.		b.d.	0.10	0.33
H ₂ O				5.67	16.2	6.48
Σ(-O=F ₂)	79.7	79.05	80.59	92.93	100.98	99.86

Note: (1–4) Glass quenched at 640°C and 2.5 kbar. Phase composition of inclusions: (1, 2) glass + unmelted crystals; (3, 4) glass + unmelted crystals + gas; (5) glass of melt A inclusions in quartz from pegmatites of Saxony [3]; (6) average composition of homogeneous glass of melt inclusions in topaz from the Volyn pegmatites [2]. The results obtained by the SIMS analysis (Cameca IMS-4f, Institute of Microelectronics, Yaroslavl; S.A. Simakin, analyst) are shown by bold font; other results were obtained with a Camebax-Micro microprobe at the Institute of Mineralogy and Petrography, Novosibirsk; L.N. Pospelova, analyst. (b.d.) Below detection limit.

the residual melt crystallized within a temperature range from no lower than 615°C to 550–500°C. Experimental data and thermodynamic computation of *PVTX* properties of boric acid solutions [13] make possible to estimate the fluid pressure during MI crystallization. As follows from the calculations, when the temperature of melt inclusion with simultaneously captured melt and fluid decreases from 615°C (liquidus) to 550°C (solidus), the intra-inclusion pressure could rise by ~1.5 kbar due to the partial release of fluid dissolved in melt. The pressure increment (*P*) may be even higher if the loss of solution immediately after melt quenching is taken into account. By analogy with melt inclusions, the crystallization of B- and H₂O-rich residual melt should increase the fluid pressure in cavity. The *P* value depends on relationships between the fluid and residual melt volumes and the quantity of water released from the melt.

The composition of quenched glass and presence of topaz, as well as Cs-, F-, and, probably, B-rich micas,

in crystalline aggregates of many melt inclusions demonstrate the unusual composition of residual melts that can concentrate extremely high quantities of H₂O, B, F, and granitophile rare elements (Cs, Li, Be, Ta, and Nb). The concentration degree of these components in residual melts is one to two orders of magnitude higher relative to the bulk composition of pegmatites in the Malkhan field [8, 14]. The Cs concentration is especially high, which promoted the formation of nanpingite (a Cs-rich analogue of muscovite) so far detected only in products of MI crystallization. This mineral may also occur in mineral assemblages as individual minerals near miarolitic cavities or in outermost zones of the mica crystals. The composition of quenched glasses in melt inclusions is close to that of counterparts in quartz from B-bearing pegmatites in Saxony with respect to many components [3], but distinguished by higher Cs and Li contents and a lack of Cl, P, and Sn. The MI glass in topaz from the Volyn pegmatites [2] contains more Na, Al, Cl, and F but less Be, Li, and B (Table 3). Relative to the granite composition inclusion glasses in late pegmatitic melts are depleted in silica, and enriched in water, indicating a considerable increase of H₂O solubility in the residual pegmatite melts.

The discrepancy in mineral composition of pocket druses and daughter-mineral assemblages in melt inclusions is probably caused by the crystallization of early minerals in miarolitic cavities primarily from fluid phase, while the residual melt played subordinate role. This is particularly evident from mineral-concentrators of Cs, Sn, and P. Because Cs is preferentially incorporated into the silicate melt, Cs-rich minerals are not found in druses formed from the aqueous phase. Occurrence of cassiterite among drusy minerals indicates that Sn was mainly partitioned into the aqueous fluid. The similar behavior is also suggested to be typical of phosphorus, whose minerals are found in both druses and miarolitic cavities. Residual melts could also accumulate elsewhere within the pegmatite body in amounts sufficient for the formation of lepidolite–tourmaline–albite aggregates with pollucite, beryl, and diverse tantaloniobates. Examination of hundreds of quartz, tourmaline, beryl, and adularia plates from miarolitic cavities and chambers in pegmatites of the Malkhan field, Borshchovochnyi Ridge (eastern Transbaikalian region), central Urals, central and southwestern Pamirs, and Namibia revealed that similar melt inclusions are rather abundant, especially in root zones of crystals growing on cavity walls. The diversity of minerals in miarolitic cavities and chambers indicates a wide compositional variation of residual melts and fluids. Compositionally unusual melts similar to those described above are very interesting for the reconstruction of mineral- and ore-forming processes at the final stage of magmatic crystallization in pegmatites and deserve further comprehensive investigations.

ACKNOWLEDGMENTS

This work was supported by the Russian Foundation for Basic Research, project nos. 01-05-64677 and 03-05-64436.

REFERENCES

1. Kosukhin, O.N., Bakumenko, I.T., and Chupin, V.P., *Magmaticheskii etap formirovaniya granitnykh pegmatitov* (Magmatic Stage of Granitic Pegmatite Formation), Novosibirsk: Nauka, 1984.
2. Kovalenko, V.I., Tsareva, G.M., Naumov, V.B., *et al.*, *Petrologiya*, 1996, vol. 4, no. 3, pp. 295–309.
3. Thomas, R., Forster, H.-J., and Heinrich, W., *Contrib. Mineral. Petrol.*, 2003, no. 144, pp. 457–472.
4. *Redkometall'nye pegmatity. Granitnye pegmatity* (Rare Metal Pegmatites: Granitic Pegmatites), Zagorsky, V.E., Makagon, V.M., Shmakina, B.M., *et al.*, Eds., Novosibirsk: Nauka, 1997, vol. 2.
5. Bakumenko, I.T. and Kovalenko, S.I., in *Termobarogeokhimicheskie issledovaniya protsessov mineraloobrazovaniya* (Thermobarogeochemical Studies of Processes of Mineral Formation), Novosibirsk: Nauka, 1988, pp. 123–135.
6. Smirnov, S.Z., Peretyazhko, I.S., Prokof'ev, V.Yu., *et al.*, *Geol. Geofiz.*, 2000, vol. 41, no. 2, pp. 194–206.
7. Peretyazhko, I.S., Zagorsky, V.E., Prokof'ev, V.Yu., *et al.*, *Petrologiya*, 2000, vol. 8, no. 3, pp. 241–266.
8. Zagorsky, V.E. and Peretyazhko, I.S., *Pegmatity s samotsvetami Tsentral'nogo Zabaikal'ya* (Pegmatites with Gemstones in the Central Transbaikalian Region), Novosibirsk: Nauka, 2000.
9. Chupin, V.P. and Kosukhin, O.N., *Geol. Geofiz.*, 1982, no. 10, pp. 66–73.
10. Morgan, G.B. and London, D., *Am. Mineral.*, 1996, vol. 81, no. 9/10, pp. 1176–1185.
11. Ihinger, P.D., Hervig, R.L., and McMillan, P.F., *Rev. Miner.*, 1994, vol. 30, pp. 67–121.
12. Veksler, I.V., Thomas, R., and Schmidt, C., *Am. Mineral.*, 2002, vol. 87, pp. 775–779.
13. Peretyazhko, I.S. and Zagorsky, V.E., *Dokl. Akad. Nauk*, 2002, vol. 383, no. 6, pp. 812–817.
14. Zagorsky, V.E. and Peretyazhko, I.S., *Geol. Geofiz.*, 1992, no. 1, pp. 87–97.